Estimate the Impact of Different Heat Capacity Approximation Methods on the Numerical Results During Computer Simulation of Solidification

Robert Dyja, Elzbieta Gawronska, Andrzej Grosser, Piotr Jeruszka and Norbert Sczygiol *†‡§¶

Abstract—**The article presents the results of numerical modeling of the solidification process. We used one of the enthalpy formulations of solidification. In particular, we focused on comparing the results of calculations for various methods of the effective thermal capacity approximation used in the apparent heat capacity formulation of solidification. We have shown that the choice of one of four tested methods of approximation does not significantly affect the results and duration of the numerical simulations. Differences in the resulting temperature did not exceed a few degrees. All numerical simulations were executed on software with our solidification module.**

Keywords: enthalpy, heat capacity, solid phase, solidification, computer simulation

1 Introduction

Aluminum alloys are very interesting material widely used in industry. Modeling and computer simulation are one of the most effective methods of studying difficult problems in foundry and metallurgical manufacture. Numerical simulations are used for optimization of casting production. In many cases they are unique possible techniques for carrying out the experiments whose real statement is complicated. Computer modeling allows to define the major factors of a quality estimation of alloy castings. Simulations help to investigate interaction between solidifying casting and changes of its parameters or initial conditions. That process defines the quality of casting, and the problem of adequate modeling of foundry systems. The process mainly depends on the solution of heat equations [1].

Increasing capacity of computer memory makes it possible to consider growing problem sizes. At the same time, increased precision of simulations triggers even greater load. There are several ways to tackle this kind of problems. For instance, one can use parallel computing [2, 3], someone else may use accelerated architectures such as GPUs [4] or FPGAs [5], while another person can use special organization of computations [6, 7, 8, 9].

Solidification may take place at a constant temperature or in the temperature range [10]. If solidification occurs at a constant temperature, it is then referred to as the so-called Stefan problem or the solidification problem with zero temperatures range. Pure metals or alloys of certain specific chemical compositions (e.g. having an eutectic composition) solidify at a constant temperature. A sharp separation of the liquid phase from the solidified phase occurs in the Stefan problem. The two phases are in contact to form a solidification surface (front). Mathematical description of the Stefan problem consists of the equation of heat conduction and the so-called Stefan condition existing on the solidification surface. However, most of the metal alloys solidify in certain temperature ranges (so-called temperature intervals of solidification). The temperature at which the alloy starts to solidify is called liquidus temperature (T_l), and the temperature at which solidification ends is called solidus temperature (T_s). In the case of alloys with eutectic transformation, in which the solute concentration exceeds its maximum solubility in the solid phase, the temperature of the solidification end is the eutectic temperature. Analytical (rarely) and numerical (commonly) methods are used in the modeling of solidification process. The finite elements method (FEM) is the most commonly used numerical method, but finite difference method (FDM), boundary element method (BEM), the Monte-Carlo and other methods are also used.

The most important heat effect, occurring during solid-

*R. Dyja is with Czestochowa University of Technology, Dabrowskiego 69, PL42201 Czestochowa Tel/Fax: (48) 34 3250589 Email: robert.dyja@icis.pcz.pl

†E. Gawronska is with Czestochowa University of Technology, Dabrowskiego 69, PL42201 Czestochowa Tel/Fax: (48) 34 3250589 Email: elabizeta.gawronska@icis.pcz.pl

‡A. Grosser is with Czestochowa University of Technology, Dabrowskiego 69, PL42201 Czestochowa Tel/Fax: (48) 34 3250589 Email: andrzej.grosser@icis.pcz.pl

§P. Jeruszka is with Czestochowa University of Technology, Dabrowskiego 69, PL42201 Czestochowa Tel/Fax: (48) 34 3250589 Email: piotr.jeruszka@icis.pcz.pl

¶N. Sczygiol is with Czestochowa University of Technology, Dabrowskiego 69, PL42201 Czestochowa Tel/Fax: (48) 34 3250589 Email: norbert.sczygiol@icis.pcz.pl

ification, is the emission of (latent) heat of solidification (L). It is also the most difficult phenomenon to numerical modeling. The basic division of numerical methods of solidification modeling process relates to modeling of the latent heat emission. These methods can be divided into front-tracking methods and fixed-grid methods. Fixed-grid methods are also divided into temperature formulations (the latent heat of solidification is considered as the temperature-dependent term of heat source) and enthalpy formulations (the latent heat of solidification is considered as the temperature-dependent term of heat capacity) [11, 12, 13, 14, 15, 16]. The enthalpy methods are divided into methods in which the effective heat capacity depends on the temperature and those in which the effective heat capacity depends on the enthalpy. In our article, we have focused on solving the solidification in the temperature range with the finite element method with the use of fixed-grid methods in enthalpy formulation. We have described the comparison of different ways of approximation of heat capacity in apparent heat capacity (AHC) formulation of solidification. This paper is the extention of previous work [17].

2 Description of the Entalphy Formulation

Solidification is described by a quasi-linear equation of heat conduction, considering a term of heat source $\dot{q}$ as a latent heat of solidification:

$$\nabla \cdot (\lambda \nabla T) + \dot{q} = c\rho \frac{\partial T}{\partial t} \tag{1}$$

By entering the following designation:

$$\dot{s} = \dot{q} - c\rho \frac{\partial T}{\partial t} \tag{2}$$

equation (1) can be written as

$$\nabla \cdot (\lambda \nabla T) + \dot{s} = 0 \tag{3}$$

where $\dot{s}$ denotes generalized heat source. By introducing enthalpy, defined as:

$$h = \int_{T_{ref}}^{T} c\rho(T)\, dt \tag{4}$$

where T_{ref} is the reference temperature, and calculating the derivative with respect to the temperature:

$$\frac{dH}{dT} = c\rho(T) = c^*(T) \tag{5}$$

where c^* is the effective heat capacity. Assuming the heat source is equal to zero, the equation (3) can be converted to the form:

$$\nabla \cdot (\lambda \nabla T) = c^* \frac{\partial T}{\partial t} \tag{6}$$

All above equations form the basis of the thermal description of solidification.

2.1 The Enthalpy and The Effective Heat Capacity

The enthalpy is the sum of explicit and latent heat [18]. For the metal solidifying in the temperature range (T_s — T_l) amounts to:

$$\begin{aligned} H &= \int_{T_{ref}}^{T} c\rho_s(T)\, dT, \quad \text{for} \quad T < T_s, \\ H &= \int_{T_{ref}}^{T_s} c\rho_s(T)\, dT + \int_{T_s}^{T} (\rho_s(T)\frac{dL}{dT} + \\ &\quad + c\rho_f(T))\, dT, \quad \text{for} \quad T_s \le T \le T_l, \\ H &= \int_{T_{ref}}^{T_s} c\rho_s(T)\, dT + \\ &\quad + \rho_s(T)L + \int_{T_s}^{T_l} c\rho_f(T)\, dT + \\ &\quad + \int_{T_l}^{T} c\rho_l(T)\, dT, \quad \text{for} \quad T > T_l \end{aligned} \tag{7}$$

The integration of the expressions in Equation 7 gives

$$\begin{aligned} c^* &= c\rho_s, \quad \text{for} \quad T < T_s, \\ c^* &= c\rho_f + \rho_s \frac{dL}{dT}, \quad \text{for} \quad T_s \le T \le T_l, \\ c^* &= c\rho_l, \quad \text{for} \quad T > T_l. \end{aligned} \tag{8}$$

Assuming that the heat of solidification is exuded and spread evenly throughout the temperature range of solidification, the following can be written:

$$\begin{aligned} c^* &= c\rho_s, \quad \text{for} \quad T < T_s, \\ c^* &= c\rho_f + \rho_s \frac{L}{T_l - T_s}, \quad \text{for} \quad T_s \le T \le T_l, \\ c^* &= c\rho_l, \quad \text{for} \quad T > T_l. \end{aligned} \tag{9}$$

On the basis of the Equation 7 and the Equation 9 one can make the following graphical comparison of the enthalpy

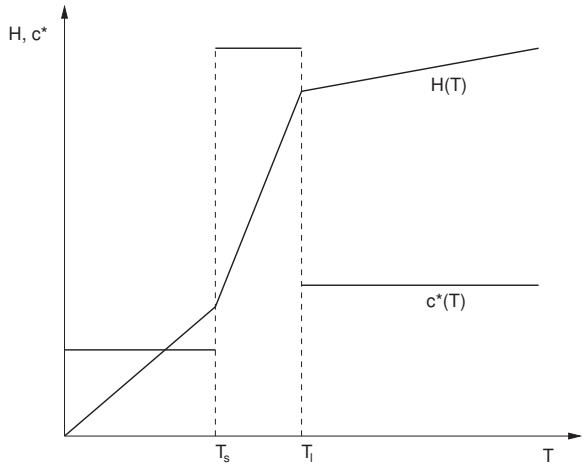

Figure 1: Distribution of enthalpy and effective heat capacity depending on temperature.

and the effective thermal capacity distributions for alloy solidifying in the temperature range (see Figure 1).

2.2 The Types of the Entalphy Formulations

There are three types of enthalpy formulations of solidification:

- basic enthalpy formulation (BEF)

$$\nabla \cdot (\lambda \nabla T) = \frac{\partial H}{\partial t} \tag{10}$$

where

$$H(T) = \int_{T_{ref}}^{T} c\rho \, dT + (1 - f_s(T))\rho_s L \tag{11}$$

- apparent (or modified) heat capacity (AHC) formulation

differentiate Eq. 11 with respect to temperature is obtained

$$\frac{dH}{dT} = c\rho - \rho_s L \frac{df_s}{dT} = c^*(T) \tag{12}$$

Since $H = H(T(\boldsymbol{x}, t))$ then

$$\frac{\partial H}{\partial t} = \frac{dH}{dT}\frac{\partial T}{\partial t} = c^*(T)\frac{\partial T}{\partial t} \tag{13}$$

Substituting Eq. 13 to Eq. 10 is obtained

$$\nabla \cdot (\lambda \nabla T) = c^*(T)\frac{\partial T}{\partial t} \tag{14}$$

- source term formulation (STF)

The total enthalpy is divided into two parts in accordance with:

$$H(T) = h(T) \, + \, (1 - f_s)\rho_s L \tag{15}$$

where

$$h(T) = \int_{T_{ref}}^{T} c\rho \, dT \tag{16}$$

Derivative Eq. 15 with respect to time is

$$\frac{\partial H}{\partial t} = \frac{\partial h}{\partial t} - \rho_s L \frac{\partial f_s}{\partial t} \tag{17}$$

Substituting Eq. 17 to Eq. 10 is obtained

$$\nabla \cdot (\lambda \nabla T) + \rho_s L \frac{\partial f_s}{\partial t} = \frac{\partial h}{\partial t} \tag{18}$$

3 Approximation of the Effective Heat Capacity

The effective heat capacity can be also calculated directly from the Equation 5, but in this paper, we have presented the results of solidification simulations using the various methods of effective heat capacity approximation.

1. Morgan method – derivative of enthalpy is replaced by a backward differential quotient

$$c^* = \frac{H^n - H^{n-1}}{T^n - T^{n-1}} \tag{19}$$

where $n-1$ and n are the time levels. In some cases, however, this substitution may lead to oscillations in the solution, especially near the boundaries of the temperature range of solidification.

2. Del Giudice method – in order to remove oscillations one should take into account the directional cosines of temperature gradient

$$c^* = \frac{\dfrac{\partial H}{\partial n}}{\dfrac{\partial T}{\partial n}} = \frac{\dfrac{\partial H}{\partial x_i}\alpha_{ni}}{\dfrac{\partial T}{\partial n}}$$

where

$$\alpha_{ni} = \frac{\dfrac{\partial T}{\partial x_i}}{\dfrac{\partial T}{\partial n}}$$

and

$$\frac{\partial T}{\partial n} = \left(\frac{\partial T}{\partial n} \cdot \frac{\partial T}{\partial n}\right)^{\frac{1}{2}}$$

Hence

$$c^* = \frac{\dfrac{\partial H}{\partial x}\dfrac{\partial T}{\partial x} + \dfrac{\partial H}{\partial y}\dfrac{\partial T}{\partial y} + \dfrac{\partial H}{\partial z}\dfrac{\partial T}{\partial z}}{(\dfrac{\partial T}{\partial x})^2 + (\dfrac{\partial T}{\partial y})^2 + (\dfrac{\partial T}{\partial z})^2} = \frac{H_{,i}T_{,i}}{T_{,j}T_{,j}} \quad (20)$$

3. Lemmon method – the temperature gradient is normal to solidification surface

$$c^* = \sqrt{\frac{\left(\frac{\partial H}{\partial x}\right)^2 + \left(\frac{\partial H}{\partial y}\right)^2 + \left(\frac{\partial H}{\partial z}\right)^2}{\left(\frac{\partial T}{\partial x}\right)^2 + \left(\frac{\partial T}{\partial y}\right)^2 + \left(\frac{\partial T}{\partial z}\right)^2}} = \left(\frac{H_{,i}H_{,i}}{T_{,j}T_{,j}}\right)^{\frac{1}{2}} \quad (21)$$

4. Comini method – the apparent heat capacity is approximated by the expression

$$c^* = \frac{1}{n}\left(\frac{\dfrac{\partial H}{\partial x}}{\dfrac{\partial T}{\partial x}} + \frac{\dfrac{\partial H}{\partial y}}{\dfrac{\partial T}{\partial y}} + \frac{\dfrac{\partial H}{\partial z}}{\dfrac{\partial T}{\partial z}}\right) = \frac{1}{n}\frac{H_{,i}}{T_{,i}} \quad (22)$$

where n is the number of dimensions.

4 Numerical model of solidification

Solving the partial differential equations can pass from spatial discretization through time discretization to approximate solution. First, we use the finite element method.

The finite element method facilitates the modeling of many complex problems. Its wide application for founding comes from the fact that it permits an easy adaptation of many existing solutions and techniques of solidification modeling.

Computer calculations need to use discrete models, which means problems must be formulated by introducing time-space mesh. These methods convert given physical equations into matrix equations (algebraic equations). This system of algebraic equations usually contains many thousands of unknowns, that is why the efficiency of a method applied to solve them is crucial.

The semi-discretization of the governing equation leads to the ordinary differential equation with time derivative, given as:

$$\mathbf{M}(T)\dot{\mathbf{T}} + \mathbf{K}(T)\mathbf{T} = \mathbf{b}(T) \quad (23)$$

where $\mathbf{M}$ is the capacity matrix, $\mathbf{K}$ is the conductivity matrix, $\mathbf{T}$ is the temperature vector and $\mathbf{b}$ is the right-hand side vector, whose values are calculated on the boundary conditions basis. The global form of these matrices is obtained by summing the coefficients for all the finite elements. The matrix components are defined for a single finite element as follows:

$$\mathbf{M} = \sum_e \int_\Omega c^* \mathbf{N}^T \mathbf{N}\, \mathrm{d}\Omega, \quad (24)$$

$$\mathbf{K} = \sum_e \int_\Omega \lambda \nabla^T \mathbf{N} \cdot \nabla \mathbf{N}\, \mathrm{d}\Omega, \quad (25)$$

$$\mathbf{b} = \sum_e \int_\Gamma \mathbf{N}_\Gamma^T \mathbf{q}^T \mathbf{n}\, \mathrm{d}\Gamma\,, \quad (26)$$

where $\mathbf{N}$ is a shape vector in the area Ω, $\mathbf{N}_\Gamma$ is a shape vector on the boundary Γ, $\mathbf{n}$ is an ordinary vector towards the boundary Γ, and $\mathbf{q}$ is a vector of nodal fluxes.

Next, we have applied one of the one-step Θ time integration schemes [19]:

- modified Euler Backward (unconditionally stable)

$$(\mathbf{M}^n + \Delta t \mathbf{K}^n)\,\mathbf{T}^{n+1} = \mathbf{M}^n \mathbf{T}^n + \Delta t \mathbf{b}^{n+1}, \quad (27)$$

where superscript n refers to following step of computations.

5 Used software of engineering simulation

Growth of computing power allows engineers to design and run engineering simulations on PC. Researchers can use typical engineering software (some kind of CAD etc.), but some of physical phenomena may not be implemented in such software. Authors decided to write their own solidification computing module, because it made computing each method of heat capacity approximation possible. The module was written in C++ programming language. We used the C++ for the module should be fast, scalable and compatible with chosen numerical utilities.

Both GMSH mesh generator and extended (to include our module) TalyFEM library have been used in numerical experiment [20]. GMSH is a widespread tool which allows finite element mesh of problem geometry (declared or created with graphical interface by user) to be generated. Furthermore, the boundary conditions (surfaces and/or volumes) can be declared with the pre-procesor using the graphical user interface.

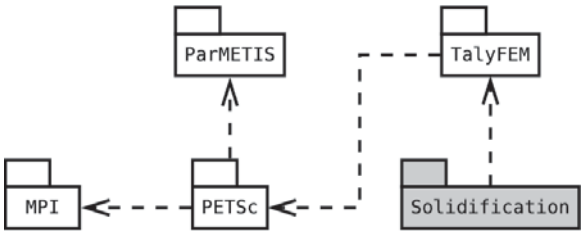

Figure 2: Package diagram in TalyFEM project.

TalyFEM is a scalable and extensible framework which uses FEM method to simulate some of physical phenomenon. TalyFEM contains many of PETSc data stuctures, including vectors, matrices or solvers [21]. PETSc library is easy to learn which allows programmers to use mentioned structures in building scalable scientific application. Scalable means using parallel techniques (provided by MPI) but a programmer does not have to write MPI communication routine — all communication about vectors and solvers is written in PETSc and TalyFEM [22]. ParMETIS (for nodes splitting) was also used in our GMSH loading file module (Fig. 2). TalyFEM also divides whole problems into sub-meshes (called domains) — each sub-problem can be solved on a separate process (processor or computer node in cluster; Fig. 3).

Hovewer, the framework does not allow to load meshes generated with GMSH pre-procesor. We wrote a GMSH loader module using MPI to communicate the data between processes. Two problems occur:

- loading material properties (which nodes belongs to a cast or an alloy);
- loading neighbourhood nodes (on contact boundary condition) if both nodes are on separate processes;

which have been solved during implementation.

We also implemented solidification module with Taly FEM library. The library requires numerical model of problem solver to be implemented. A programmer does not have to write matrices of the assembly code or communication routines – they are provided with the library. Nevertheles, we considered parameters of boundary conditions (especially contact boundary condition), so we modified standard modules of filling matrices while we were creating the system of linear equations. Framework also solves the created equations (by mentioned communication routines) and writes them into output files (in TecPlot format).

6 Results of the Numerical Experiment

In the paper we considered a casting solidifying in a metal mold. The finite element mesh comprising 32 814 nodes and 158 417 elements was applied to the area of the casting and mold, as shown in Figure 4. We introduced two boundary conditions: Newton and continuity condition, for which the environment temperature 400 K, the heat transfer coefficient with the environment 10 W/m^2K^{-1} and the heat transfer coefficient through the separation layer 1000 W/m^2K^{-1} are definied. The initial temperature of casting was 960 K, the initial temperature of mold was 600 K, the size of the time step was 0.05 s.

Material properties of the alloy (of which the casting is made of) and the mold are given in Tables 1 and 2, respectively.

Figure 4 shows the distribution of temperatures in the casting after 25 s for the Morgan heat capacity approximation.

The graphs in Figures 5 and 7 show the lack of differences in the obtained results. We can see that cooling curves and solid fractions of all methods overlap. It is caused by the fact that although different heat capacity approximations use different formulas, the resulting approximations are very close in values of effective heat capacity, as can be seen in Figure 6.

However, there is a visible difference between the heat capacity approximation formulas in calculation times. The Figure 8 shows the difference in assembly time for different methods. It is easy to notice that the Morgan method requires the least time, while the other formulas are close together in time requirement.

The results from the Figure 8 were obtained for 750 time-steps and mesh from Figure 1. On the 750th time-step (after 37.5 s) the minimum solid fraction was still 0.95 (see Fig. 7). This ensures that during the whole calculation time in at least some fraction of finite elements the heat capacity approximation formulas were used.

7 Conclusions

By analyzing the numerical results obtained from calculations carried out with the help of our own computer program using the finite element method and the apparent heat capacity method we can draw the following remarks and conclusions:

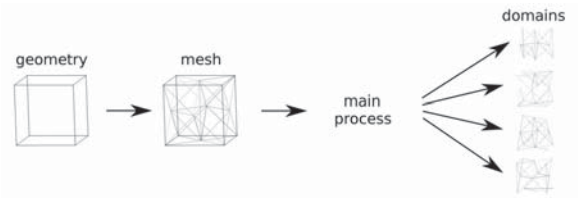

Figure 3: Splitting whole problem to domains in TalyFEM GMSH loader module.

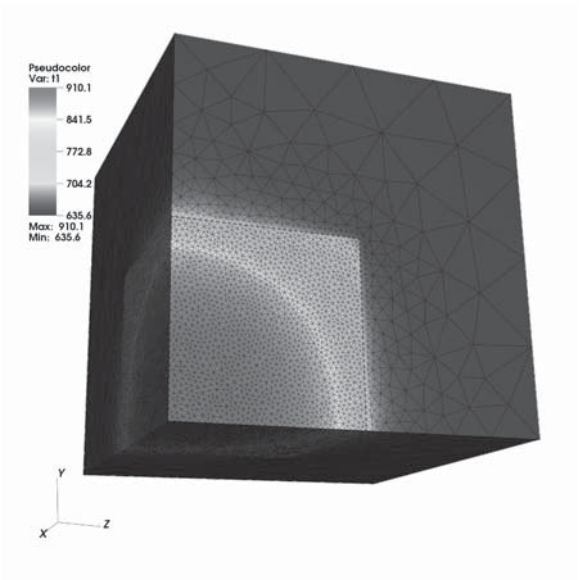

Figure 4: Temperature field after 25 s of cooling. The Finite Element mesh is also visible.

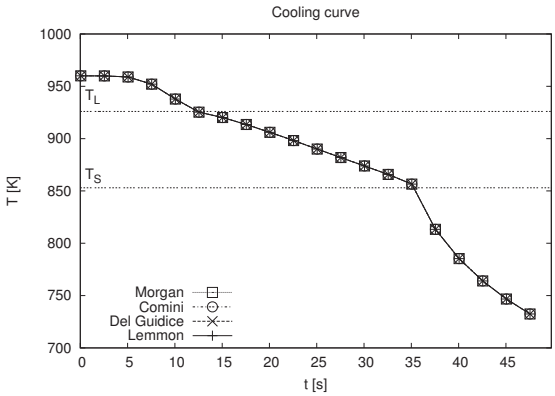

Figure 5: A cooling curve of a point located in origin of coordinate system.

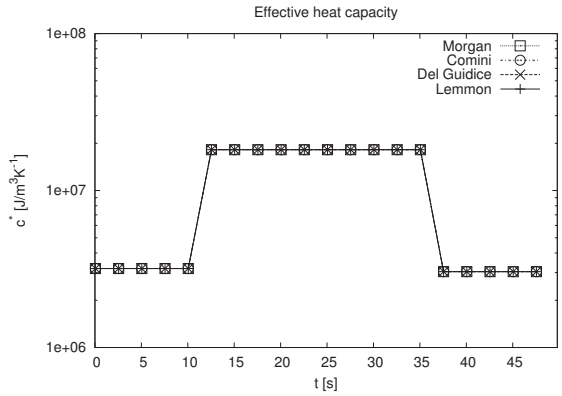

Figure 6: The change of heat capacity approximate during solidification process.

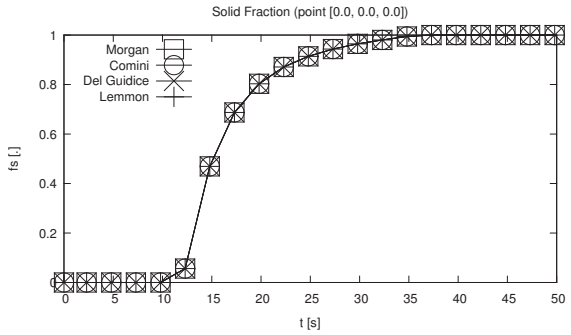

Figure 7: Curve of the solid phase fraction in point (0,0,0).

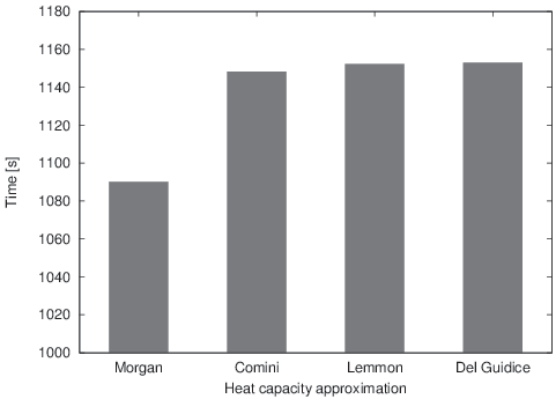

Figure 8: The difference between the heat capacity approximation formulas in time needed for the main matrix assembly.

Table 1: Material properties of the Al-2%Cu alloy (subscript s means solid phase and l – liquid phase)

Quantity name	**Unit**	**Value**
Density ρ_s	$\frac{kg}{m^3}$	2824
Density ρ_l	$\frac{kg}{m^3}$	2498
Specific heat c_s	$\frac{J}{kgK^{-1}}$	1077
Specific heat c_l	$\frac{J}{kgK^{-1}}$	1275
Thermal conductivity λ_s	$\frac{W}{mK^{-1}}$	262
Thermal conductivity λ_l	$\frac{W}{mK^{-1}}$	104
Solidus temperature T_s	K	853
Liquidus temperature T_l	K	926
Melt temperature of pure component T_M	K	933
Eutectic temperature T_E	K	821
Heat of solidification L	$\frac{J}{kg}$	390 000
Partition coefficient of solute k	—	0.125

Table 2: Material properties of the mold

Quantity name	**Unit**	**Value**
Density	$\frac{kg}{m^3}$	7500
The specific heat	$\frac{J}{kgK^{-1}}$	620
Thermal conductivity coefficient	$\frac{W}{mK^{-1}}$	40

1. The capacity formulation gives an equation very similar to the equation of heat conduction; heat of solidification is hidden in the effective thermal capacity.

2. The use of any of the heat capacity approximation methods does not affect the obtained result, if the solution is stable.

3. When using the Morgan method of heat capacity approximation, one should be careful not to apply too small time step, because then the obtained results might be incorrect.

4. Heat capacity approximation formulas other than Morgan are susceptible to give wrong results if temperature values in nodes of one finite element differ by very small values. The Comini method is especially sensitive to this.

5. Morgan method requires the least time for calculations.

References

[1] D. M. Stefanescu, *Science and Engineering of Casting Solidification*, New York: Kluwer Academic, 2002

[2] R. Wyrzykowski, L. Szustak, and K. Rojek, "Parallelization of 2d mpdata eulag algorithm on hybrid architectures with gpu accelerators", *Parallel Computing*, V40, N8, pp. 425–447, 2014

[3] J. W. Kim and R. D. Sandberg, "Efficient parallel computing with a compact finite difference scheme", *Computers & Fluids*, V58, pp. 70–87, 2012

[4] G. Michalski and N. Sczygiol, "Using CUDA architecture for the computer simulation of the casting solidification process", in *Proceedings of the International MultiConference of Engineers and Computer Scientists*, Hong Kong: Lecture Notes in Engineering and Computer Science, pp. 933–937, 03/2014

[5] N. Yang, D. W. Li, J. Zhang, and Y. G. Xi, "Model predictive controller design and implementation on FPGA with application to motor servo system", *Control Engineering Practice*, V20, N11, pp. 1229–1235, 2012

[6] E. Gawronska and N. Sczygiol, "Numerically Stable Computer Simulation of Solidification: Association Between Eigenvalues of Amplification Matrix and Size of Time Step", in *Transactions on Engineering Technologies*, Springer Netherlands, pp. 17–30, 2015

[7] E. Gawronska and N. Sczygiol, "Relationship between eugenvalues and size of time step in computer simulation of thermomechanics phenomena", in *Proceedings of the International MultiConference of Engineers and Computer Scientists*, Hong Kong: Lecture Notes in Engineering and Computer Science, pp. 881–885, 03/2014

[8] A. Ghoneim and O.A. Ojo, "Numerical modeling and simulation of a diffusion-controlled liquidsolid phase change in polycrystalline solids", *Computational Materials Science*, V50, N3, pp.1102–1113, 2011

[9] E. Gawronska and N. Sczygiol, "Application of mixed time partitioning methods to raise the efficiency of solidification modeling", *12th International Symposium on Symbolic and Numeric Algorithms For Scientific Computing (SYNASC 2010)*, pp. 99–103, 2010

[10] F. Stefanescu, G. Neagu, A. Mihai, I. Stan, M. Nicoara, A. Raduta, and C. Opris, "Controlled temperature distribution and heat transfer process in the unidirectional solidification of aluminium alloys",

Advanced Materials and Structures IV, V188, pp. 314–317, 2012

[11] A. W. Date, "A novel enthalpy formulation for multidimensional solidification and melting of a pure substance", *Sadhana-Academy Proceedings in Engineering Sciences*, V19, pp. 833–850, 1994

[12] Q. Duan, F. L. Tan, and K. C. Leong, "A numerical study of solidification of n-hexadecane based on the enthalpy formulation", *Journal of Materials Processing Technology*, V120, N1/3, pp. 249–258, 2002

[13] S. Ganguly and S. Chakraborty, "A generalized formulation of latent heat functions in enthalpy – based mathematical models for multicomponent alloy solidification systems", *Metallurgical and Materials Transactions B-Process Metallurgy and Materials Processing Science*, V37, N1, pp. 143–145, 2006

[14] A. J. Prabha, S. Raju, B. Jeyaganesh, A. K. Rai, et al., "Thermodynamics of $\alpha^{''} \rightarrow \alpha$ phase transformation and heat capacity measurements in Ti15at%Nb alloy", *Physica B*, V406, N22, pp. 4200–4209, 2011

[15] M. Famouri, M. Jannatabadi, and H. T. F. Ardakani, "Simultaneous estimations of temperature-dependent thermal conductivity and heat capacity using a time efficient novel strategy based on megann", *Applied Soft Computing*, V13, N1, pp. 201–210, 2013

[16] R. Dyja, N. Sczygiol, Z. Domanski, S. Ao, A. Chan, H. Katagiri, and L. Xu, "The effect of cavity formation on the casting heat dissipation rate", in *IAENG Transactions on Engineering Sciences*, pp. 341–347, 2014

[17] R. Dyja, E. Gawroska, A. Grosser. P. Jeruszka, N. Sczygiol, "Comparison of different heat capacity approximation in solidification modeling", in *Lecture Notes in Engineering and Computer Science*, World Congress on Engineering and Computer Science, WCECS 2015, 21-23 October, San Francisco, USA, V2, pp. 875-879, 10/2015

[18] N. Sczygiol and G. Szwarc, "Application of enthalpy formulation for numerical simulation of castings solidification", *Computer Assisted Mechanics and Engineering Sciences*, N8, pp. 99–120, 2001

[19] L. W. Wood, *Practical Time-stepping Schemes*, Oxford: Clarendon Press, 1990

[20] H.K. Kodali, B. Ganapathysubramanian, "A computational framework to investigate charge transport in heterogeneous organic photovoltaic devices", *Computer Methods in Applied Mechanics and Engineering*, N247, pp. 113–129, 2012

[21] Balay S. et al., *PETSc Users Manual*, Argonne National Laboratory, 2014

[22] MPI: A Message Passing Interface, *http://www.mpi-forum.org*, mpi30-report.pdf, 15.03.2016 r.